Application of continuation methods in physical oceanography

C.A. Katsman [†‡], H.A Dijkstra[‡] and M.J. Schmeits[‡]

January 21, 1999

Abstract

A specific example will be considered in which continuation methods are used to study fundamental problems in physical oceanography. The separation behavior of the Gulf Stream in the North Atlantic is a long standing problem in dynamical oceanography, with state-of-the-art ocean models still having trouble to simulate to correct mean path. Bifurcation analysis in simplified models, as used here, points to one of difficulties involved: there may be two separation paths at the same forcing conditions. By studying the stability of steady North Atlantic ocean circulation patterns, also transitions to time-dependence are found which are linked to specific low frequency variability in the Gulf Stream region.

1 Introduction

1.1 Ocean Circulation and Climate

Since the beginning of this century, an enormous amount of data has been gathered on the state of the different components of the climate system. Simultaneously, a large database is also being generated through all kinds of proxy data, obtained, for example from tree rings and oxygen isotope ratios in ocean sediment and ice cores. Using the latter data, signatures of the state of the climate system in the (far) past can be reconstructed.

All these observations indicate that climate fluctuates on a broad range of time scales. Of current interest are the climate fluctuations on interannual to interdecadal time scales (Kushnir, 1994), because of their role in distinguishing natural from possible antropogenic induced climate changes. Within climate research, a relevant question is the origin of this natural variability and the key physical processes causing it. It is by now clear that the ocean and in particular its circulation is centrally involved on a large range of – from intermonthly to millenial – time scales.

On the large scale, the ocean circulation is driven by wind forcing and by fluxes of heat and freshwater at the ocean-atmosphere interface. A classical picture of the wind-driven surface circulation is shown in Fig. 1. Major features are the peculiar equatorial

current system, with an eastward equatorial countercurrent between westward equatorial currents in both Atlantic and Pacific, the Antartic Circumpolar Current, which encircles the Antartic continent from west to east and the cellular (gyre) type circulation at midlatitudes. In the North-Atlantic, a most prominent feature is the Gulf Stream which can be viewed as an eastward jet being part of two gyres, the so-called subtropical and subpolar gyre. These gyre-type circulations are also seen in the North Pacific, with the same east-west asymmetry and a strong western-boundary current, the Kuroshio, near Japan.

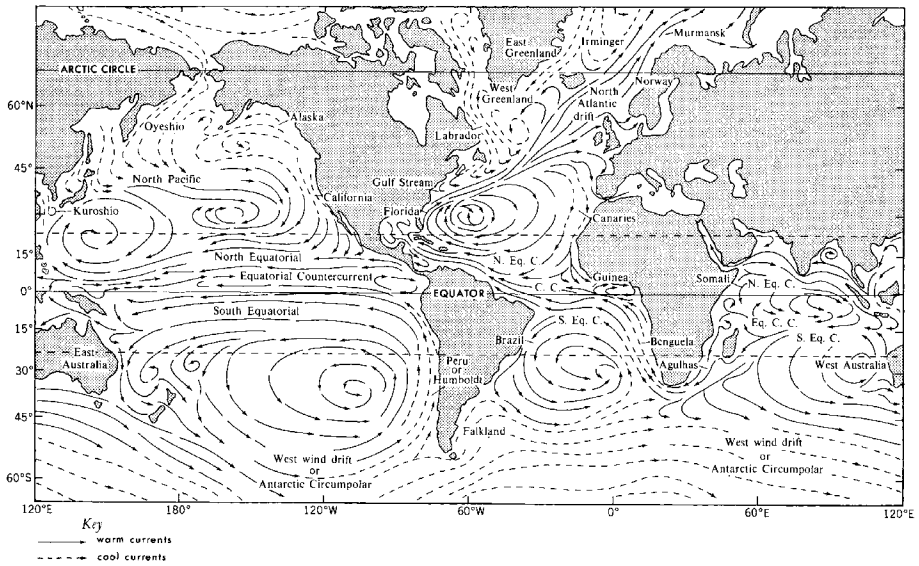

Figure 1: *Sketch of the global surface (wind-driven) ocean circulation (after Peixoto and Oort (1992))*

The circulation driven by density gradients, caused by gradients in temperature and salinity, is called the thermohaline circulation. The relatively warm and saline water transported by the Gulf Stream is cooled on its way northward. In certain regions, i.e. the Greenland and Labrador Sea, the water column becomes unstably stratified and vigorous convection occurs. The net effect is the formation of a relatively cold and fresh water mass (called the North Atlantic Deep Water) which is transported southward at mid-depth as a (deep) western boundary current. This deep flow crosses the equator and connects to the watermasses of the Southern Ocean. Together, the wind-driven and thermohaline circulation form a complex three dimensional flow of different watermasses through the ocean basins, with different levels of coherence on different scales, which has been termed (Gordon, 1986; Broecker, 1991) the 'Ocean Conveyor' (Fig. 2). Its properties are not well-determined yet, because of a lack of observations over the whole globe, in particular in the deep ocean.

In general, the ocean moderates climate through its large thermal inertia, its capacity to store enormous amounts of heat and its poleward heat transport through

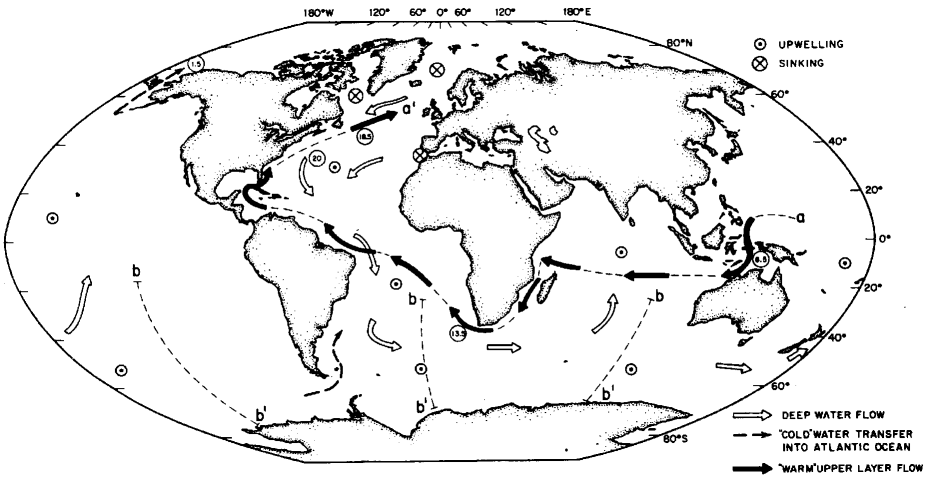

Figure 2: *Sketch of the global ocean circulation: the 'Ocean Conveyor'. In this figure, sites of deep water formation are indicated by crosses and the dots indicate upwelling areas (after (Gordon, 1986))*

ocean currents. Hence, changes in the currents, which may involve only one current systems or a reorganization of the global flow, can induce significant changes in the climate system. The subtle changes in the North Atlantic surface circulation and their interactions with the overlying atmosphere are certainly involved in the intermonthly through interdecadal climate variability as observed over the last century; the work here is motivated by latter variability.

1.2 The Gulf Stream

Most important current in the North Atlantic Ocean is the Gulf Stream. The southern part of the Stream (the Florida Current) flows almost parallel to the coastline (Fig. 3). At Cape Hatteras the Gulf Stream leaves the North-American continent and moves further eastward along $40°W$. It appears that the position of the separation point is quite stable, changing less than about 50 $[km]$ over several years. Further into the open ocean the Gulf Stream spreads out due to meandering and displays an enormous amount of variability. In this area, eddies are found which move away from the mainstream generally in westward/southwestward direction. Their average wavelength is about 100 $[km]$ and propagation speeds of these eddies are about 10 $[km/day]$.

In early days, the variability of the Gulf Stream was studied using in-situ data but more recently these data have been complemented with satellite derived observations. Using infrared images for the period April 1982 through December 1989, Lee and Cornillon (1995) found two dynamically distinct modes of variability of the path of the Gulf Stream. The first mode of variability is associated with large-scale lateral shifts of the mean path having a near-annual period. These shifts are presumably caused by atmospheric forcing, through the changes in downward heat flux over the area. The

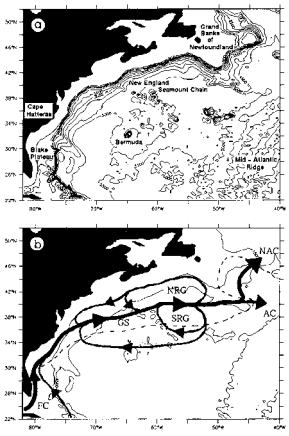

Figure 3: *(a) Geography and bathymetry of Gulf Stream region (after Dengg* et al. *(1996)). (b) Sketch of the near surface circulation. Bold lines: Florida Current (FC) and Gulf Stream (GS), branching into the North Atlantic Current (NAC) and Azores Current (AC) (after (Dengg, 1993))*

second mode of variability is associated with changes in meandering intensity having a 9-month dominant periodicity. The cause of the 9-month periodicity in meandering intensity is unclear but is proposed in Lee and Cornillon (1995) to be related to internal oceanic dynamics.

Both the mean path as well as the spatial and temporal patterns of its variability are central to understand the changes in meridional heat transport of the Gulf Stream. It is these two different themes which have been focus of theoretical research over the last decades, encompassing work using numerical models and more fundamental theory to which we turn next.

2 An intermediate ocean model

Consider a flat-bottomed ocean basin with a realistic horizontal domain $\mathcal{V}$ and bounded by a closed contour Γ. Apart from neglecting bottom topography, also the stratification is not considered and the density of the ocean is constant. The flow is driven by a windstress $\tau(\phi, \theta) = \tau_0(\tau^\phi, \tau^\theta)$, where τ_0 is the amplitude and (τ^ϕ, τ^θ) provides the spatial pattern. Laplacian lateral friction, with lateral friction coefficient A_H, is the dissipative mechanism in the model. In the usual notation, the velocities in eastward and northward directions are indicated by u and v, respectively and h is the thickness of the water column (with equilibrium value D). The latter changes due to variations in the sea surface height.

In principle, the governing equations are the incompressible Navier-Stokes equations on the sphere. However, because a typical layer thickness is much smaller than the horizontal dimensions of the flow, the shallow water approximation can be made. The final

equations are obtained by integration over the layer (Pedlosky, 1987). The governing shallow water equations are non-dimensionalized using scales $r_0, D, U, r_0/U$ and τ_0 for length, layer depth, velocity, time and windstress, respectively, where r_0 is the radius of the earth and U is a characteristic horizontal velocity. They can be written in latitude θ and longitude ϕ as

$$\epsilon\left(\frac{\partial u}{\partial t}+\frac{u}{cos\theta}\frac{\partial u}{\partial \phi}+v\frac{\partial u}{\partial \theta}-uvtan\theta\right)-$$
$$-vsin\theta=-\frac{\epsilon F}{cos\theta}\frac{\partial h}{\partial \phi}+E\left(\nabla^2 u-\frac{u}{cos^2\theta}-\frac{2sin\theta}{cos^2\theta}\frac{\partial v}{\partial \phi}\right)+\alpha\frac{\tau^\phi}{h} \tag{1a}$$
$$\epsilon\left(\frac{\partial v}{\partial t}+\frac{u}{cos\theta}\frac{\partial v}{\partial \phi}+v\frac{\partial v}{\partial \theta}+u^2tan\theta\right)+$$
$$+usin\theta=-\epsilon F\frac{\partial h}{\partial \theta}+E\left(\nabla^2 v-\frac{v}{cos^2\theta}+\frac{2sin\theta}{cos^2\theta}\frac{\partial u}{\partial \phi}\right)+\alpha\frac{\tau^\theta}{h} \tag{1b}$$
$$\frac{\partial h}{\partial t}+\frac{1}{cos\theta}\left(\frac{\partial (hu)}{\partial \phi}+\frac{\partial (hvcos\theta)}{\partial \theta}\right)=0 \tag{1c}$$

On the boundary Γ of the domain no-slip conditions are prescribed, i.e.

$$(\phi,\theta)\ \varepsilon\ \Gamma: \quad u=v=0 \tag{2}$$

The parameters in these equations are the Rossby number ϵ, the Froude number F, the Ekman number E, and the windstress coefficient α. Expressions for these parameters are

$$\epsilon=\frac{U}{2\Omega r_0}\ ;\ F=\frac{gD}{U^2}\ ;\ E=\frac{A_H}{2\Omega r_0^2}\ ;\ \alpha=\frac{\tau_0}{2\Omega\rho DU} \tag{3}$$

where Ω is the angular velocity of the earth and g the gravitational acceleration. Standard values of the parameters in this model are listed in Table 1.

3 Numerical methods

3.1 Discretization of the equations

The governing equations are written as

$$M(\frac{\partial \mathbf{u}}{\partial t})=L(\mathbf{u})+N(\mathbf{u},\mathbf{u}) \tag{4}$$

where $\mathbf{u}=(u,v,h)^T$ is the solution vector, M and L are linear operators and N is the nonlinear operator. A domain $[\phi_W,\phi_E]\times[\theta_S,\theta_N]$ over the globe is chosen and an equidistant staggered grid is defined by gridpoints $i,j,\ \cdots, i=1,I, j=1,J$, with u and

Dimensional parameters			
Parameter	Value	Parameter	Value
r_0	$6.37 \times 10^6\ m$	τ_0	$1.5 \times 10^{-1}\ Pa$
D	$1.0 \times 10^3\ m$	A_H	$2.0 \times 10^2\ m^2\ s^{-1}$
g	$9.8\ m\ s^{-2}$	U	$1.0 \times 10^{-1}\ m\ s^{-1}$
ρ_0	$1.0 \times 10^3\ kg\ m^{-3}$	Ω	$7.3 \times 10^{-5} s^{-1}$
Dimensionless parameters			
Parameter	Value	Parameter	Value
α	1.0×10^{-2}	E	3.4×10^{-8}
ϵ	1.1×10^{-4}	F	9.8×10^5

Table 1: *Standard values of dimensional and dimensionless parameters in the shallow water model*

v at the middle of east-west and north-south boundaries of the domain and h-points at the center of the grid cell. Next a standard bathymetry data set is used to define an array of land points and ocean point for the chosen domain and resolution. The forcing of the ocean circulation τ is also obtained from a standard data set of the annual averaged winds and interpolated on the center points of the grid. Standard central differencing is used on this staggered grid leading to a system of nonlinear algebraic equations at each point of the domain on the sphere. If grid centers are land points, the governing equations at that location are changed and u, v and h-point are zeroed. The no-slip boundary conditions at other boundaries are taken into account through second order central differencing.

3.2 Steady states

To compute steady states, a (large dimensional) system of nonlinear coupled algebraic equations of the form

$$\mathbf{F}(\mathbf{x}, \mathbf{p}) = L(\mathbf{x}) + N(\mathbf{x}, \mathbf{x}) = 0 \tag{5}$$

has to be solved. Here $\mathbf{x}$ is the discrete solution vector and $\mathbf{p}$ the vector of parameters. Solutions of the equations (5) are traced in parameter space using a pseudo-arclength method (Keller, 1977). With λ as control parameter, branches $(\mathbf{x}(s), \lambda(s))$ are parameterized by an arclength parameter s. An additional equation follows from the normalization of the tangent along the branch, i.e. (with the dot denoting differentiation to s),

$$\dot{\mathbf{x}}_0^T(\mathbf{x} - \mathbf{x}_0) + \dot{\lambda}_0(\lambda - \lambda_0) - \Delta s = 0 \tag{6}$$

In the equation above, $(\mathbf{x}_0, \lambda_0)$ is an analytically known starting solution or a previously computed point on a particular branch and Δs is the step length. To solve the

system of equations (5, 6) Euler-Newton continuation is used.

Within the Newton-Raphson process, each iteration constists of the following $\mathbf{x}^{k+1} = \mathbf{x}^k + \Delta\mathbf{x}$ where k indicates the iteration step. To find $\Delta\mathbf{x}$, use is made of

$$\frac{\partial \left[L(\mathbf{x^k}) + N(\mathbf{x}^k, \mathbf{x}^k)\right], \mathbf{x}}{\partial \Delta}\mathbf{x} = -(L(\mathbf{x}^k) + N(\mathbf{x}^k, \mathbf{x}^k)) \tag{7}$$

Because of the quadratic nonlinearity, this system can be written in terms of matrix vector multiplications and eventually, systems of the form

$$\left(L + N_J(\mathbf{u}^k)\right)(\Delta\mathbf{u}) = -\left(L + N_R(\mathbf{u}^k)\right)(\mathbf{u}^k) \tag{8}$$

are solved, with appropriate definitions of N_J and N_R. For example, for the term $u\partial_x u$ in the equations,

$$N_J(\mathbf{u}^k) = \partial_x \mathbf{u}^k + \mathbf{u}^k \partial_x \tag{9a}$$

$$N_R(\mathbf{u}^k) = \partial_x \mathbf{u}^k \tag{9b}$$

3.3 Linear stability

The linear stability analysis of a computed steady state amounts to solving a generalized eigenvalue problem of the form

$$\beta\mathcal{A}\mathbf{x} = \alpha\mathcal{B}\mathbf{x} \tag{10}$$

where $\mathcal{A}$ is a real non-singular, non-symmetric matrix. Through the boundary conditions and/or the continuity constraint, $\mathcal{B}$ is singular. In the latter case, $\beta = 0$ for at least one eigenvalue; if $\beta \neq 0$, then the eigenvalue problem σ is found from α/β. In earlier versions of the code (**?**), the Simultaneous Iteration Technique was used after a Cayley transformation was applied to map the spectrum left of the imaginary axis into the unit circle.

In the new version of the code, two other eigenvalue solvers have been implemented. The first is the Arnoldi method available within the ARPACK (**?**) software and the second is the recently developed Jacobi-Davidson QZ method (**?**). The latter method combines subspace iteration with the construction of generalized Schur vectors and its implementation in the continuation code BAGELS is described in **?**).

3.4 Solution of the linear systems

For both the computation of the steady states as well as the determination of its linear stability, linear systems have to be solved. A robust method is the direct solution through Gauss elimination with partial pivoting. For the banded matrices which appear this is an option, when band solvers are used, for example, as implemented in the NAG library.

Since the direct solvers are soon memory limiting and no high resolution can be achieved, also iterative solvers are implemented. Both Bi-CGSTAB Van der Vorst (1992) and $GMRES$ (**?**) are used as the basic iterative method for the solution of these linear systems. As in general, the matrices are not well-conditioned, the linear system is preconditioned first before the iterative method is applied.

As preconditioners, variants of incomplete LU-decomposition are used. The first type implemented is where the construction of the incomplete decomposition is based on sparsity pattern of $L + U$ and a drop tolerance ε_p. The construction of the factors L, U and the choice of ε_p is described in detail in Van der Ploeg (1992). In order to increase the efficiency of the incomplete decomposition, it is possible to perform a renumbering of the unknowns which is based on the same basic idea as in multi grid methods. Recently, also the MRILU method, as presented elsewhere in this book has been implemented.

When several systems of linear equations have to be solved in which the coefficient matrices do not differ very much, as in continuation methods such as used here, it is possible to use the same preconditioner many times.

3.5 Detection of special points

To monitor simple bifurcation points on a particular branch, several indicator functions are used. For example, limit points are detected by following $\dot{\lambda}$. For transcritical or pitchfork bifurcations, the sign of the determinant of the Jacobian may be used, but this quantity is only available if a direct linear solver is used. When this determinant is not readily available, in the case when iterative solvers are used, a family of test functions τ_{pq} is implemented following Seydel (1979). For the computation of each test function τ_{pq}, one additional linear system has to be solved. Other singularities, like Hopf bifurcation points, must be detected by solving the linear stability problem.

4 Typical results

@ Maybe add picture on the wind forcing chosen.

The bifurcation diagram for standard values of parameters is shown in Figure 4a using the Ekman number E as control parameter. On the vertical axis, the maximum northward volume transport in Sv, 1 $Sv = \ 10^6\ m^3/s$ is plotted. Two solution branches are found, on which solutions are unstable for $E < 2.5 \times 10^{-7}$, and the topology of the branches is a perturbed pitchfork bifurcation (Golubitsky and Schaeffer, 1985).

A solution on the lower branch is shown as a contour plot of h for $E = 1.6 \times 10^{-7}$ in Figure **??**b. It displays the double gyre circulation, typical for the North-Atlantic Ocean, although the Gulf Stream separates too far north, compared to reality. Moreover, there is a weak southern recirculation region and at this value of E the transport ϕ is about $46Sv$. The other branch exists only for $E < 2.2 \times 10^{-7}$, which is the position of the turning point on this branch. The solution at $E = 1.6 \times 10^{-7}$ (Fig. **??**c) displays a Gulf

Stream that separates two times. The first time it separates too far south, compared to reality, and the second time too far north (at about the same latitude as in Figure 4b). There is now a strong southern recirculation region. At this value of E, the transport ϕ is about 70 Sv, which is 1.5 times larger than that in Figure 4b, and somewhat larger than current estimates near Cape Hatteras of about 50-65 Sv. By comparing Figure 4b and **??**c, it can be concluded that the circulation patterns outside the region of the western boundary current are very similar, so that the multiple equilibria correspond to multiple mean paths of the Gulf Stream near its separation region.

On the lower branch in Figure 4a, a Hopf bifurcation occurs at $E = 2.5 \times 10^{-7}$ and is marked with H_1. At H_1 the steady state becomes unstable to one oscillatory mode. The pattern of this mode is determined from the eigenvector $\mathbf{x} = \mathbf{x}_r + i\mathbf{x}_i$ associated with the eigenvalue $\sigma = \sigma_r + i\sigma_i$ in (10). These span an oscillatory mode given by

$$\Psi(t) = \exp(\sigma_r t)\{\cos(\sigma_i t)\,\mathbf{x}_r - \sin(\sigma_i t)\,\mathbf{x}_i\} \tag{11}$$

with dimensional period $T = 2\pi r_0/(U\sigma_i)$.

The perturbation is shown at two phases within half a period of the oscillation in Figure 5a-b. The mode is located around the axis of the western boundary current and propagates southwestward, i.e. upstream. It has a period of 6 months, a wavelength of about 550 km and a maximum amplitude of 9 mm. From Figure 5a-b we can deduce that the perturbation adds cross-stream components to the flow in the western boundary current, i.e. it causes the Gulf Stream to meander.

To investigate the sensitivity of the results to the layer thickness D, a regime diagram was computed (Fig. 6a). At each value of D, the linear stability boundary is determined by the value of E at the Hopf bifurcation H_1. It is obvious from Figure 6a that the circulation gets more stable as D increases. This is a result of the fact that the same energy input by the windstress forcing is distributed over a deeper layer, which stabilizes the flow. The spatial pattern of the neutral mode does not change with D, but the period of the oscillation increases from 6 to 11 months in the range of D considered (Figure 6b).

The bifurcation diagram of the perturbed pitchfork and the regime diagram of its transition to oscillatory behavior demonstrates that internal ocean dynamics can give rise to different mean states under the same forcing conditions and that it can induce preference for some frequencies of variability.

5 Summary

Main result of the application of continuation techniques to the wind-driven ocean circulation in the North-Atlantic is the existence of multiple mean paths of the Gulf Stream. For one of these solutions, the overshooted solution, separation is very diffuse and occurs at the wrong location. The other 'separated' solution shows a better mean path of the Gulf Stream. For the model used here, the correct separated solution exists, but small friction is required to be able to reach this solution. At small enough friction,

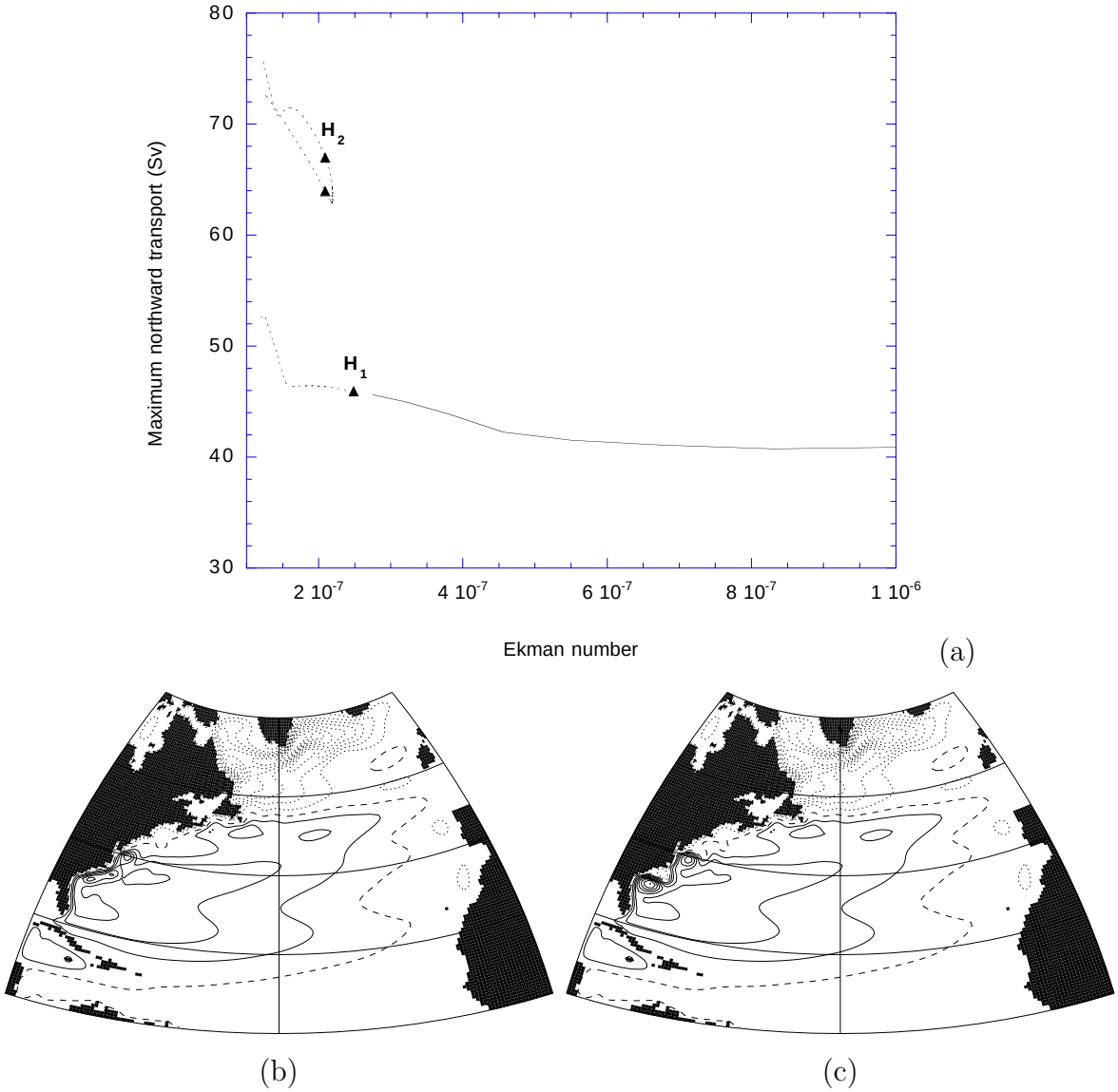

Figure 4: *Bifurcation diagram for the realistic case, using the Ekman number as control parameter; drawn (dotted) branches indicate stable (unstable) steady states. (b) Contour plot of the layer thickness anomaly for the 'deflected' Gulf Stream at* $E = 3.0 \times 10^{-6}$. *(c) Contour plot of the layer thickness anomaly for the 'separated' Gulf Stream at* $E = 3.0 \times 10^{-6}$.

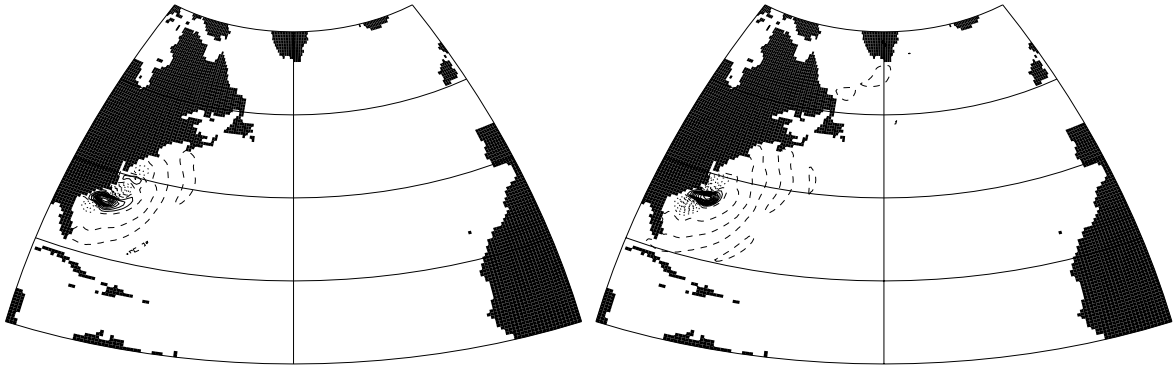

(a) (b)

Figure 5: *Eigenfunctions corresponding to the unstable mode at the marked points in Fig. 4a for* $E = 3.0\ 10^{-6}$*; shown are the layer thickness perturbations. (a-b): Real and imaginary part of the unstable oscillatory mode on the steady state shown in Fig.* **??***b, with* $\sigma_r = 2.2yr^{-1}$ *and* $\sigma_i = 16.1yr^{-1}$.

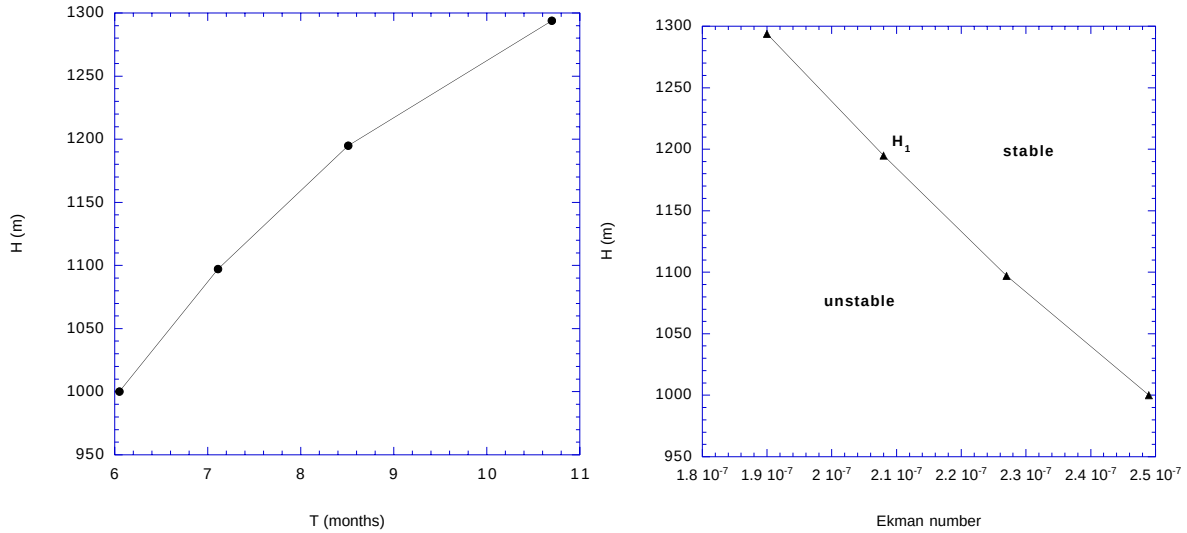

(a) (b)

Figure 6:

the steady states become unstable to oscillatory modes which consists of propagating disturbances along the Gulf Stream. The modes are prototypes to explain the variability in the meandering intensity of the Gulf Stream.

Ocean general circulation models (OGCM's), having a realistic continental geometry and bathymetry and incorporating the thermohaline circulation, are run now with an eddy-resolving resolution, not only for the Atlantic (New *et al.*, 1996). These results also show large internal variability on a wide range of time scales and the influence of the eddies on the mean flow. The interpretation of results of these models is not without problems, because of the multitude of physical effects which can influence a phenomenon under study. For example, it appears that several physical processes control the mean flow path of the Gulf Stream, in particular its separation near Cape Hatteras. In models of 1° horizontal resolution (Holland and Bryan, 1994), separation of the Gulf Stream is very diffuse between Cape Hatteras and Newfoundland and no recirculation regions are present. For very high resolution models of $\frac{1}{6}^\circ$ (Beckmann *et al.*, 1994; Bryan *et al.*, 1995) the time mean state shows a large anti-cyclonic gyre north of Cape Hatteras giving an actual separation north of the observed position with non-desirable consequences for the simulated heat transport.

Results of this study using a model with obviously enormous simplifications first indicates why large scale ocean models may have trouble to obtain the correct mean separated path of the Gulf Stream. Two possible separation paths may actually exist and the more realized path is only found in the model for small enough friction. Hence, if the horizontal resolution of the ocean models is not high enough they may not to be able to deal with small enough friction and no correct separation is found. Second, the study of the identification of modes of variability has just begon, focussing on the 9 month variability in the meander intensity (Schmeits and Dijkstra, 1999).

6 Acknowledgments

All computations were performed on the CRAY C90 at the Academic Computing Centre (SARA), Amsterdam, the Netherlands. Use of these computing facilities was sponsored by the National Computing Facilities Foundation (NCF) with financial support from the Netherlands Organization for Scientific Research (NWO). The work of MS and HD was supported by an NWO PIONIER grant (030-76-187) to H.D. and that of CK was supported through NWO grant ....

References

Beckmann, A., Böning, C. W., Köberle, J., and Willebrand, J. (1994). Effects of increased horizontal resolution in a simulation of the North-Atlantic ocean. *J. Phys. Oceanography*, **24**, 326–344.

Broecker, W. S. (1991). The great ocean conveyor. *Oceanography*, **4**, 79–89.

Bryan, F. O., Böning, C. W., and Holland, W. (1995). On the midlatitude circulation in a high-resolution model of the North-Atlantic. *J. Phys. Oceanography*, **25**, 289–305.

Dengg, J. (1993). The problem of Gulf Stream separation: A barotropic approach. *J. Phys. Oceanography*, **23**, 2182–2200.

Dengg, J., Beckmann, A., and Gerdes, R. (1996). The Gulf Stream separation problem. In W. A. Kraus, editor, *The warmwatersphere of the North Atlantic Ocean*, pages 253–290. Borntraeger.

Golubitsky, M. and Schaeffer, D. G. (1985). *Singularities and groups in bifurcation theory*. Springer-Verlag.

Gordon, A. (1986). Interocean exchange of thermocline water. *J. Geophysical Res.*, **91**, 5037–5046.

Holland, W. R. and Bryan, F. (1994). Modelling the wind and thermohaline circulation in the North-Atlantic Ocean. In P. Malanotte-Rizzoli and A. Robinson, editors, *Ocean processes in Climate Dynamics: Global and Mediterranean examples*, pages 35–156. Kluwer Academic, Netherlands.

Keller, H. B. (1977). Numerical solution of bifurcation and nonlinear eigenvalue problems. In P. H. Rabinowitz, editor, *Applications of bifurcation theory*. Academic Press.

Kushnir, Y. (1994). Interdecadal variations in north atlantic sea surface temperature and associated atmospheric conditions. *J. Phys. Oceanography*, **7**, 141–157.

Lee, D. and Cornillon, P. (1995). Temporal variation of meandering intensity and domain-wide lateral oscillations of the Gulf Stream. *J. Geophysical Res.*, **100 C7**, 13,603–13,613.

New, A. L., Bleck, R., Jia, Y., Marsh, M., Huddleston, M., and Barnard, S. (1996). An isopycnic model study of the North Atlantic. Part 1: Model experiment and water mass formation. *J. Phys. Oceanography*, **26**, 253–278.

Pedlosky, J. (1987). *Geophysical Fluid Dynamics*. Springer-Verlag, New York.

Peixoto, J. and Oort, A. (1992). *Physics of Climate*. AIP Press.

Schmeits, M. and Dijkstra, H. (1999). On the physics of the 9 months variability in the gulf stream region: combining data and dynamical systems analysis. *J. Phys. Oceanography*.

Seydel, R. (1979). Numerical computation of branch points in nonlinear equations. *Num. Math.*, **33**, 339–352.

Van der Ploeg, A. (1992). Preconditioning techniques for non-symmetric matrices with application to temperature calculations of cooled concrete. *Int. J. Num. Methods Eng.*, **35(6)**, 1311–1328.

Van der Vorst, H. A. (1992). Bi-CGSTAB: A fast and smoothly converging variant of bi-cg for the solution of nonsymmetric linear systems. *jpo*, **23**, 39–60.